Progress of Theoretical Physics, Vol. 81, No. 6, June 1989

q-Phase Transitions in Chaotic Attractors of Differential Equations at Bifurcation Points

Koji TOMITA, Hiroki HATA, Takehiko HORITA, Hazime MORI, Terumitsu MORITA, Hisao OKAMOTO and Hirotaka TOMINAGA

Department of Physics, Kyushu University 33, Fukuoka 812

(Received December 24, 1988)

Most nonlinear ordinary differential equations exhibit chaotic attractors which have singular local structures at their bifurcation points. By taking the driven damped pendulum and the Duffing equation, such chaotic attractors are studied in terms of the q-phase transitions of a q-weighted average $\Lambda(q)$, $(-\infty<q<\infty)$ of the coarse-grained expansion rates Λ of nearby orbits along the unstable manifolds. We take their Poincaré maps in order to obtain the expansion rates Λ and their spectrum $\psi(\Lambda)$ explicitly. It is shown that q-phase transitions occur at crises in the differential equations. Just before the crises, q_β-phase transitions occur due to the collisions of the attractors with unstable periodic orbits. Numerical values of the transition points q_β thus obtained agree fairly well with theoretical predictions. q_δ-phase transitions occur just after the crises where the chaotic attractors are suddenly spread over chaotic repellers. Thus it turns out that the q-phase transitions of Λ(q) are useful for characterizing the chaotic attractors of differential equations at their bifurcation points.

§ 1. Introduction

In the analysis of dissipative dynamical systems, most attention has been given to the characterization of chaotic attractors. In particular, scaling properties of chaotic attractors have been studied from the metric and the dynamic point of view.[1)~6)] In a series of papers,[7)~12)] we have shown for universal maps such as the logistic and Hénon maps that the singular local structures of chaotic attractors created at their bifurcations produce remarkable linear slopes in the spectrum $\psi(\Lambda)$ of the coarse-grained expansion rates Λ of nearby orbits along the unstable manifolds, which bring about the q-phase transitions of the q-weighted average $\Lambda(q)$ of Λ.

Let us summarize the theoretical framework developed in the previous papers.[7)~12)] Let $\{\boldsymbol{X}_m\}$, $(m=0, 1, 2, \cdots)$ be a chaotic orbit on a chaotic attractor generated by a $2d$ (i.e., two-dimensional) Poincaré map $\boldsymbol{X}_{m+1}=\boldsymbol{F}(\boldsymbol{X}_m)$, and define the coarse-grained expansion rates

$$\Lambda_n(\boldsymbol{X}_0)\equiv(1/n)\sum_{m=0}^{n-1}\lambda_1(\boldsymbol{X}_m) \tag{1·1}$$

for large n, where $\lambda_1(\boldsymbol{X}_m)$ is the local expansion rate of nearby orbits at $\boldsymbol{X}_m$ along the unstable manifold. We assume that the attractor is ergodic. Then as $n\to\infty$, $\Lambda_n(\boldsymbol{X}_0)$ converges to a positive Liapunov number Λ^∞ for almost all initial points $\boldsymbol{X}_0$ within the basin of attraction of the chaotic attractor. The probability density for $\Lambda_n(\boldsymbol{X}_0)$ to take a value around Λ is given by

$$P(\Lambda; n)\equiv\langle\delta(\Lambda_n(\boldsymbol{X}_0)-\Lambda)\rangle\,, \tag{1·2}$$

where $\delta(g)$ is the δ-function of g and $\langle\cdots\rangle$ denotes the long-time average

$$\langle G(\boldsymbol{X}_0)\rangle \equiv \lim_{N\to\infty}(1/N)\sum_{t=0}^{N-1} G(\boldsymbol{X}_t)\,. \tag{1·3}$$

Then $P(\Lambda; n)$ would take the scaling form[13]

$$P(\Lambda; n)=\exp\{-n\psi(\Lambda)\}P(\Lambda^{\infty}; n) \tag{1·4}$$

for $n\to\infty$, where $\psi(\Lambda)\geq\psi(\Lambda^{\infty})=0$. This defines the spectrum $\psi(\Lambda)$ which is a concave function and describes the fluctuations of $\Lambda_n(\boldsymbol{X}_0)$ around Λ^{∞}. Numerically, the probability density (1·2) was computed for a finite n by taking a large but finite N in the long-time average (1·3). Then $\psi(\Lambda)$ was approximated by

$$\psi_n(\Lambda)\equiv -(1/n)\ln[P(\Lambda; n)/P(\Lambda^{\infty}; n)] \tag{1·5}$$

with $\Lambda^{\infty}=\langle\Lambda_n(\boldsymbol{X}_0)\rangle$.

In order to describe large fluctuations of Λ explicitly, we also used the dynamic partition function

$$Z_n(q)\equiv\int d\Lambda\, P(\Lambda; n)\exp\{-n(q-1)\Lambda\}\,, \qquad (-\infty<q<\infty) \tag{1·6}$$

and the temporal scaling exponents[2)~6)]

$$\Phi_n(q)\equiv -(1/n)\ln Z_n(q)\,, \tag{1·7}$$

$$\Lambda_n(q)\equiv d\Phi_n(q)/dq\,, \qquad \sigma_n(q)\equiv -d\Lambda_n(q)/dq\geq 0\,. \tag{1·8}$$

The functions (1·5)~(1·8) are called the dynamic structure functions. Inserting (1·4) into (1·6) and taking the largest integrand for large n, we obtain the variational principle

$$\Phi_n(q)=\min_{\Lambda}\{\psi(\Lambda)+(q-1)\Lambda\} \tag{1·9}$$

for large n, where $\psi'(\Lambda)=1-q$ leads to an approximation $\Lambda(q)$ for $\Lambda_{\infty}(q)$.

At the bifurcation points such as crises,[14] chaotic attractors have singular local structures, so that $\psi(\Lambda)$ has a linear slope $s_t=1-q_t$, $(t=\alpha, \beta, \cdots)$ which brings about the q-phase transition of $\Lambda_{\infty}(q)$ at $q=q_t$.[10] Each phase of the q-phase transition represents different local structures of the chaotic attractors. For example, the q_{β}-phase transition is caused by the collision of the chaotic attractor with an unstable periodic orbit $\{\boldsymbol{S}_i\}$ at a crisis point which is accompanied by the accumulation of heteroclinic or homoclinic tangency points at the periodic orbit.[9),10)] Then the two phases of the q_{β}-phase transition represent the hyperbolic structures and the tangency structures, respectively.

It would be important to see how the above idea of the q-phase transitions developed for simple $2d$ maps such as the Hénon map is also valid for the ordinary differential equations which are the usual description of dynamical laws in the physical science. We shall take the driven damped pendulum and the Duffing equation. Since the $\lambda_1(\boldsymbol{X}_m)$'s in (1·1) are defined for $2d$ maps, we shall take the Poincaré maps for these differential equations. We shall numerically obtain the dynamic structure functions at some crises and clarify that the q_{β}- and q_{δ}-phase transitions occur just before and after the crises, respectively.

In § 2 two crises of the driven damped pendulum are studied. In § 3 we describe results for the Duffing equation. The last section is devoted to a short summary and some remarks.

§ 2. Driven damped pendulum

We consider the equation of motion for the driven damped pendulum

$$\ddot{\theta}+\gamma\dot{\theta}+\sin\theta=a\cos(\Omega t)\,, \tag{2·1}$$

where θ is the pendulum angle, γ is the damping constant, a and Ω are the amplitude and angular frequency of the driving periodic torque. This equation also gives a useful model for the radiofrequency-driven Josephson junctions and the charge density wave in semiconductors, and it has recently been studied extensively for various values of the parameters a, γ and Ω to clarify its chaotic behaviors.[15)~17)]

The phase space of the system is the $3d$ Euclidean space spanned by $x=\theta$, $y=\dot{\theta}$ and $\varphi=\Omega t \pmod{2\pi}$ with

$$\dot{x}=y\,,\quad \dot{y}=-\gamma y-\sin x+a\cos\varphi\,, \tag{2·2a}$$

$$\dot{\varphi}=\Omega\,. \pmod{2\pi} \tag{2·2b}$$

Therefore any orbit in this phase space intersects the $\varphi=0$ plane at time $t_m=2\pi m/\Omega$, $(m=0, 1, 2, \cdots)$ so that the $\varphi=0$ plane provides the Poincaré section with intersections $\boldsymbol{X}_m\equiv\{x(t_m), y(t_m)\}$, leading to a Poincaré map $\boldsymbol{X}_{m+1}=\boldsymbol{F}(\boldsymbol{X}_m)$.

First we take $\gamma=1/\sqrt{15}$, $\Omega=0.65$ and a in the vicinity of a crisis value

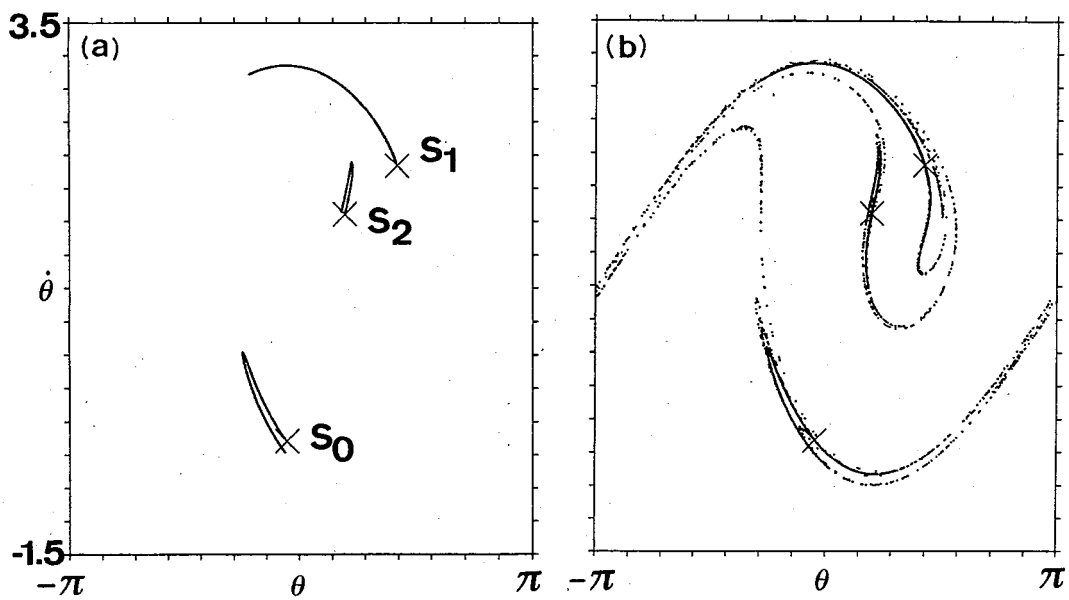

Fig. 1. Chaotic attractor of the pendulum (2·1) near the crisis point $a=a_w\simeq 0.728384$ with $\gamma=1/\sqrt{15}$ and $\Omega=0.65$. The period-3 saddles are shown by crosses ×. (a) Just before the crisis ($a=a_w-0$). (b) Just after the crisis ($a=a_w+0$).

$a_w \simeq 0.728384$. For a slightly less than a_w, there is a three-time rolled attractor whose Poincaré section is a confined three-band attractor shown in Fig. 1(a). At $a=a_w$ the attractor touches the stable manifold of an unstable periodic orbit $\{S_0, S_1, S_2\}$ with period $(2\pi/\Omega)\times 3$ which is indicated by crosses $\times$ in Fig. 1. This crisis is homoclinic.[14] As a increases beyond a_w, the attractor is widened like Fig. 1(b).

In order to obtain the dynamic structure functions $\psi_n(\Lambda)$, $\Lambda_n(q)$ and $\sigma_n(q)$, we have to consider the Poincaré map $\boldsymbol{X}_{m+1}=\boldsymbol{F}(\boldsymbol{X}_m)$ and get the local expansion rate

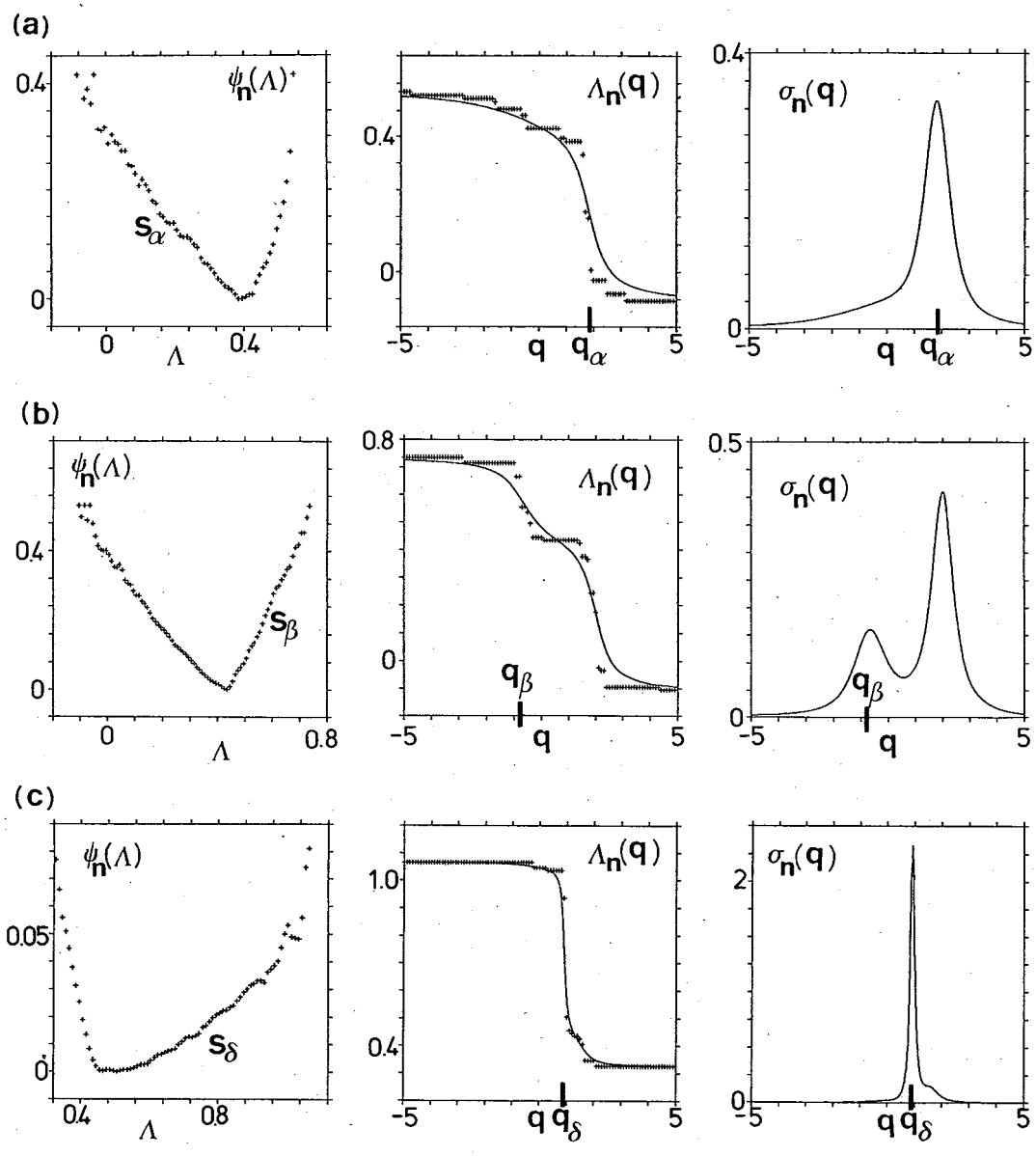

Fig. 2. Dynamic structure functions for the pendulum (2·1) around the crisis point $a=a_w$ with $\gamma=1/\sqrt{15}$ and $\Omega=0.65$. (a) Far from the crisis, where $a=0.728$, $n=18$, $N=1.28\times10^5$. (b) Just before the crisis, where $a=0.7283832$, $n=21$, $N=1.6\times10^6$. (c) Just after the crisis, where $a=0.7288$, $n=100$, $N=3.2\times10^5$.

$\lambda_1(\boldsymbol{X}_m)$ along the unstable manifold at $\boldsymbol{X}_m$. Therefore, taking an initial point $\boldsymbol{X}_0=\{x(t_0), y(t_0)\}$ and a unit vector $\{\xi(t_0), \eta(t_0)\}$, we numerically integrate the variation equations

$$\dot{\xi}=\eta\,, \tag{2·2c}$$

$$\dot{\eta}=-\gamma\eta-\{\cos x(t)\}\xi\,, \tag{2·2d}$$

until $t_1=2\pi/\Omega$, and then take $\lambda_1(X_0)=\ln\{|\xi(t_1)|^2+|\eta(t_1)|^2\}^{1/2}$. Then we again integrate (2·2) starting from the point $\{x(t_1), y(t_1)\}$ and the unit vector $\{\xi(t_1)/\exp[\lambda_1(\boldsymbol{X}_0)], \eta(t_1)/\exp[\lambda_1(\boldsymbol{X}_0)]\}$ till $t_2=(2\pi/\Omega)\times 2$. Then we obtain $\{x(t_2), y(t_2)\}$ and $\lambda_1(\boldsymbol{X}_1)=\ln\{|\xi(t_2)|^2+|\eta(t_2)|^2\}^{1/2}$. If we repeat this process, then the vector $\{\xi(t_m), \eta(t_m)\}$ will become tangent to the attractor which lies on the closure of an unstable manifold, so that we can get the local expansion rate $\lambda_1(\boldsymbol{X}_m)=\ln\{|\xi(t_{m+1})|^2+|\eta(t_{m+1})|^2\}^{1/2}$ along the unstable manifold. Using this $\lambda_1(\boldsymbol{X}_m)$, we obtain the coarse-grained expansion rates (1·1) and the dynamic structure functions from the formula summarized in § 1.

Figure 2(a) shows the dynamic structure functions far from the bifurcation point $a=a_w$. The crosses + for $\Lambda_n(q)$ represent the largest-term approximation obtained from the variational principle (1·9). The q-weighted variance $\sigma_n(q)$ has only one peak at $q=q_\alpha\simeq 1.81$. This peak would diverge as $n\to\infty$, ensuring that $\Lambda_\infty(q)$ exhibits the q_α-phase transition at $q=q_\alpha$ due to the homoclinic tangencies on the chaotic attractor. $\psi_n(\Lambda)$ has a linear slope $s_\alpha=1-q_\alpha\simeq -0.81$.

Just before the crisis, another q-phase transition occurs at $q=q_\beta\simeq -0.67$ as shown in Fig. 2(b), which corresponds to the linear slope $s_\beta\simeq 1.67$ of $\psi_n(\Lambda)$. This slope is theoretically given in terms of the mean expansion rate $\Lambda_\infty(\boldsymbol{S}_i)$ of the period-3 saddles $\{\boldsymbol{S}_i\}$ as follows:[9]

$$s_\beta=g\alpha_1(\boldsymbol{S}_i)\Lambda_\infty(\boldsymbol{S}_i)/\{\Lambda_\infty(\boldsymbol{S}_i)-\Lambda^0\}\,, \tag{2·3}$$

Table I. $\alpha_1(\boldsymbol{S}_i)$, $\alpha(\boldsymbol{S}_i)$ and s_β just before the crises in the driven damped pendulum (2·1) and the Duffing equation (3·1).[a]

	$\Lambda_\infty(\boldsymbol{S}_i)$	$\alpha_1(\boldsymbol{S}_i)$	$\alpha(\boldsymbol{S}_i)$	g	Λ^0	s_β	
						theor	exp
(pendulum)							
$a=a_w-0$							
$\gamma=1/\sqrt{15}$	0.880	0.676	0.852	1.115	0.45	1.54	1.67
$\Omega=0.65$							
$a=a_m-0$							
$\gamma=0.22$	0.627	0.727	0.954	1.135	0.30	1.58	1.59
$\Omega=1.0$							
(Duffing)							
$a=a_c-0$	1.310	0.847	1.195	1.170	0.41	1.44	1.24
$\gamma=0.3$							

a) The singularity exponent $\alpha_1(\boldsymbol{S}_i)$ is given by (2·5) for the homoclinic case. The total exponent is $\alpha(\boldsymbol{S}_i)=\{1+r(\boldsymbol{S}_i)\}\alpha_1(\boldsymbol{S}_i)$ with $r(\boldsymbol{S}_i)\equiv\Lambda_\infty(\boldsymbol{S}_i)/\{\Lambda_\infty(\boldsymbol{S}_i)-\ln|\boldsymbol{J}|\}$, where $|\boldsymbol{J}|=\exp(-2\pi\gamma/\Omega)$ for the pendulum (2·1) and $|\boldsymbol{J}|=\exp(-2\pi\gamma)$ for the Duffing equation (3·1).

where g and $\alpha_1(\boldsymbol{S}_i)$ are given by

$$g=1+\Lambda_\infty(\boldsymbol{S}_i)/\{3\Lambda_\infty(\boldsymbol{S}_i)+2|\ln|\boldsymbol{J}||\}\,, \tag{2·4}$$

$$\alpha_1(\boldsymbol{S}_i)=0.5+\Lambda_\infty(\boldsymbol{S}_i)/2|\ln|J||\,, \tag{2·5}$$

and Λ^0 is the value of Λ at which the extension of the linear part of $\psi(\Lambda)$ crosses the Λ-axis. J is the Jacobian of the Poincaré map, i.e. $|J|=\exp(-2\pi\gamma/\Omega)$. The numerical value $s_\delta\simeq 1.67$ is in good agreement with the theoretical estimate $s_\delta=1.54$ obtained from (2·3), as shown in Table I.

Results just after the crisis are shown in Fig. 2(c). $\sigma_n(q)$ has a sharp peak at $q=q_\delta\simeq 0.91$, so that $\Lambda_n(q)$ exhibits a q-phase transition at $q=q_\delta$ different from the above two. This phase transition occurs when the attractor begins to include a chaotic repeller. Its intuitive picture is the following. Let us suppose that just before a crisis ($a=a_w-0$) there exist an attractor and a chaotic repeller which have $\psi(\Lambda)=\psi_A(\Lambda)$ and $\psi(\Lambda)=\psi_R(\Lambda)$, respectively, as illustrated in Fig. 3(a). The minima of $\psi(\Lambda)$ are $\psi_A(\Lambda_A^\infty)=0$ and $\psi_R(\Lambda_R^\infty)=T_R^{-1}>0$, where T_R is the mean lifetime of the orbits around the repeller. Just after the crisis ($a=a_w+0$) the attractor extends over the repeller and becomes a larger attractor, so that $\psi(\Lambda)$ has a new linear part with a slope s_δ to connect $\psi_A(\Lambda)$ and $\psi_R(\Lambda)$ in the way shown in Fig. 3(b). This linear slope brings about a q_δ-phase transition with $q_\delta=1-s_\delta$.

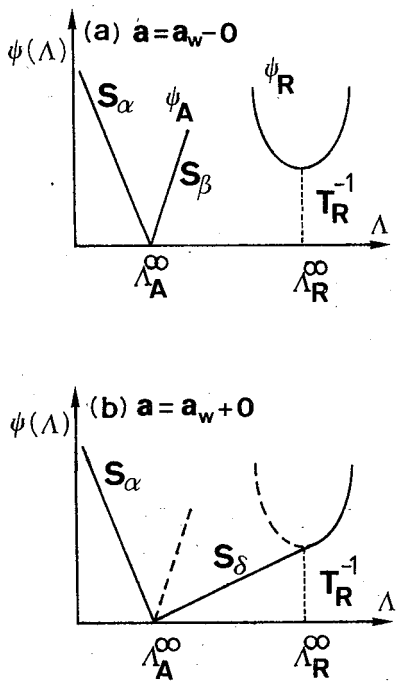

Fig. 3. Schematic illustration of $\psi(\Lambda)$ just before and after a crisis. In (a), $\psi(\Lambda)$ of an attractor and a chaotic repeller are shown. In (b), as a result of the crisis, the attractor and the repeller merge so that $\psi(\Lambda)$ comes to have a linear slope s_δ which induces the q_δ-phase transition of $\Lambda(q)$ at $q=q_\delta=1-s_\delta$.

Second, we take $\gamma=0.22$, $\Omega=1$. These parameters were used in Ref. 14), and a crisis occurs at $a=a_m=2.6465274\cdots$. Just below a_m there are two attractors with rotation numbers $\rho\equiv\langle\dot{\theta}\rangle/\Omega=1$ and $\rho=-1$. However, these two attractors must have the same scaling structures due to the symmetry of Eq. (2·1), since Eq. (2·1) is invariant under $\theta\to-\theta$, $\Omega t\to\Omega t+\pi$. At $a=a_m$, the two attractors simultaneously touch the stable manifolds of the two unstable period-6 orbits whose expansion rates are identical with each other due to the symmetry. Just past $a=a_m$ the two chaotic attractors merge to form a larger phase-unlocked attractor. Figures 4(a) and (b) illustrate the attractors just before and after the crisis, respectively. The orbital structure just before $a=a_m$ with its basin boundary is shown in Fig. 4(c). The points in the black region are attracted by the attractor with $\rho=-1$, while the points in the white region are

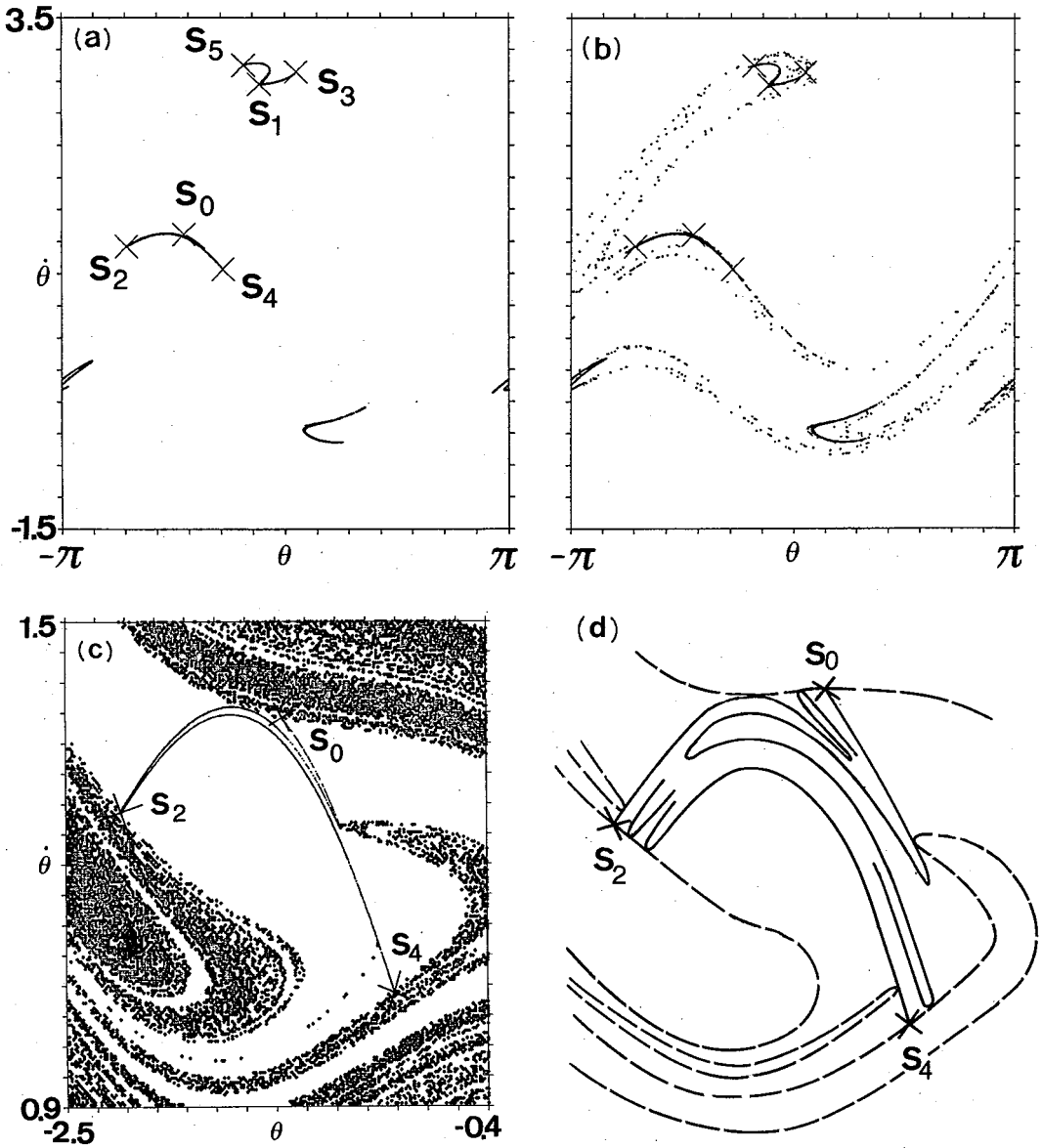

Fig. 4. Chaotic attractors of the pendulum (2·1) near the crisis point $a=a_m\simeq 2.6465274$ with $\gamma=0.22$ and $\Omega=1$. The period-6 saddles are shown by ×'s. (a) Just before the crisis. (b) Just after the crisis. (c) Basin boundary for the attractor. The points in the white region are attracted by the attractor with $\rho=1$. (d) Schematic illustration of the homoclinic tangencies of the unstable manifold (solid line) and of the stable manifold (dashed line) of the period-6 saddles (crosses). In (c) and (d) a part of the attractor with $\rho=1$ is shown.

attracted by that with $\rho=1$. Their basin boundaries are the stable manifolds of the two unstable period-6 orbits which collide with the attractors at $a=a_m$. Then, as illustrated in Fig. 4(d), the tangency points $\{\boldsymbol{X}_j\}$ accumulate at $\{\boldsymbol{S}_i\}$ marked by the crosses as $j\to\pm\infty$. Hence the crisis is homoclinic. This orbital structure is similar

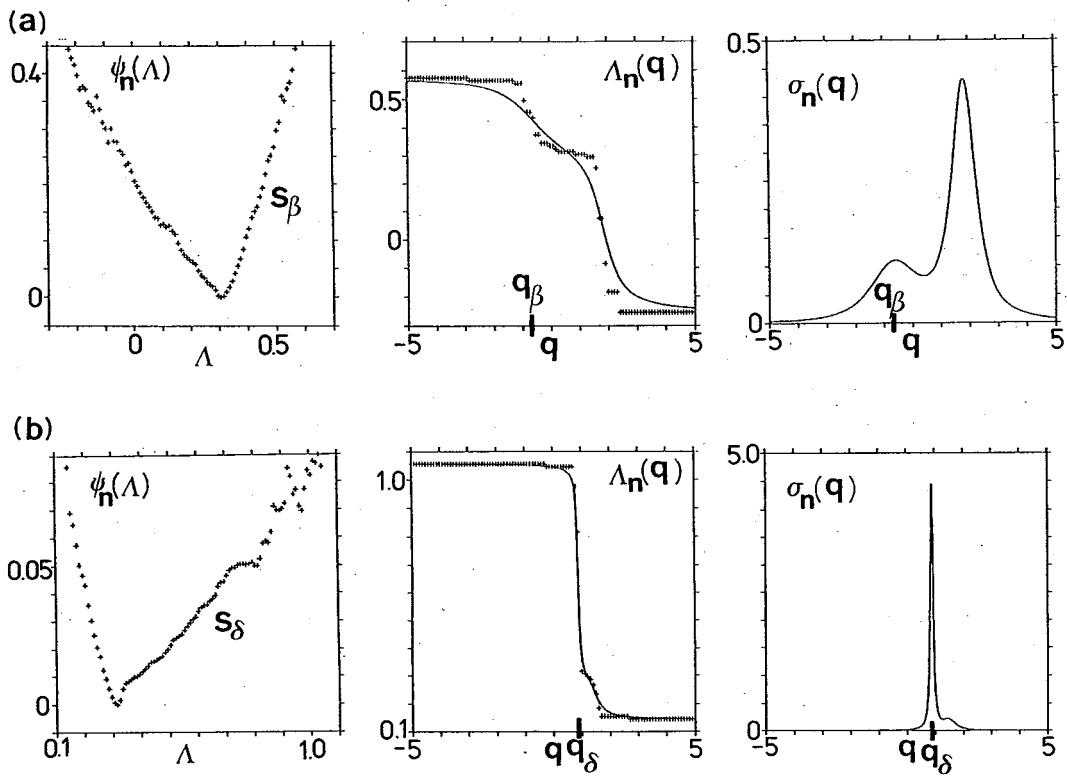

Fig. 5. Dynamic structure functions for the pendulum (2·1) near the crisis point $a=a_m$ with $\gamma=0.22$ and $\Omega=1$. (a) Just before the crisis, where $a=2.6462$, $n=18$, $N=1.28\times10^5$. (b) Just after the crisis, where $a=2.6475$, $n=100$, $N=1.28\times10^5$.

to the first case. Indeed, as shown in Fig. 5, a q_β-phase transition with $q_\beta\simeq-0.59$ occurs just before the crisis and a q_δ-phase transition with $q_\delta\simeq0.89$ occurs just after the crisis. The slope $s_\beta\simeq1.59$ of the linear part of $\psi_n(\Lambda)$ in Fig. 5(a) is in good agreement with the theoretical value $s_\beta=1.58$ obtained from (2·3), as listed in Table I.

§ 3. The Duffing equation

In this section we deal with chaotic attractors of the Duffing equation

$$\ddot{x}+\gamma\dot{x}+x^3=a\cos t\,. \tag{3·1}$$

This is a mathematical model for a series-resonance circuit, containing a saturable inductor, and for a point particle in a potential well $V(x)=x^4/4$ subjected to friction and an external periodic force. Ueda was the first who found a chaotic behavior of this equation[18] and his chaotic attractor is well known as "a Japanese Attractor".[19]

We consider a crisis which occurs at $a=a_c\simeq10.5242$, $\gamma=0.3$. Namely, as a is increased to a_c with $\gamma=0.3$, a three-band attractor approaches and collides with the period-3 saddles $\{S_i\}$, $(i=0, 1, 2)$. The orbital structures and the dynamic structure functions at the crisis are shown in Figs. 6 and 7, respectively. It is found that a

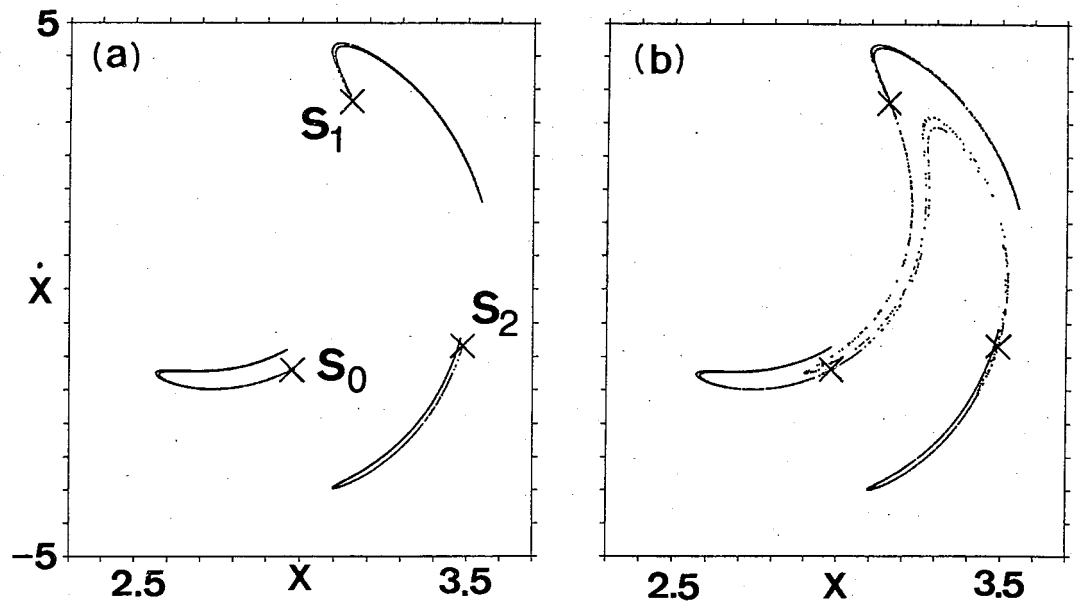

Fig. 6. Chaotic attractor of the Duffing equation (3·1) near the crisis point $a=a_c\simeq 10.5243$ with $\gamma=0.3$, together with the period-3 saddles $\{S_0, S_1, S_2\}$ marked by three ×'s. (a) Just before the crisis. (b) Just after the crisis.

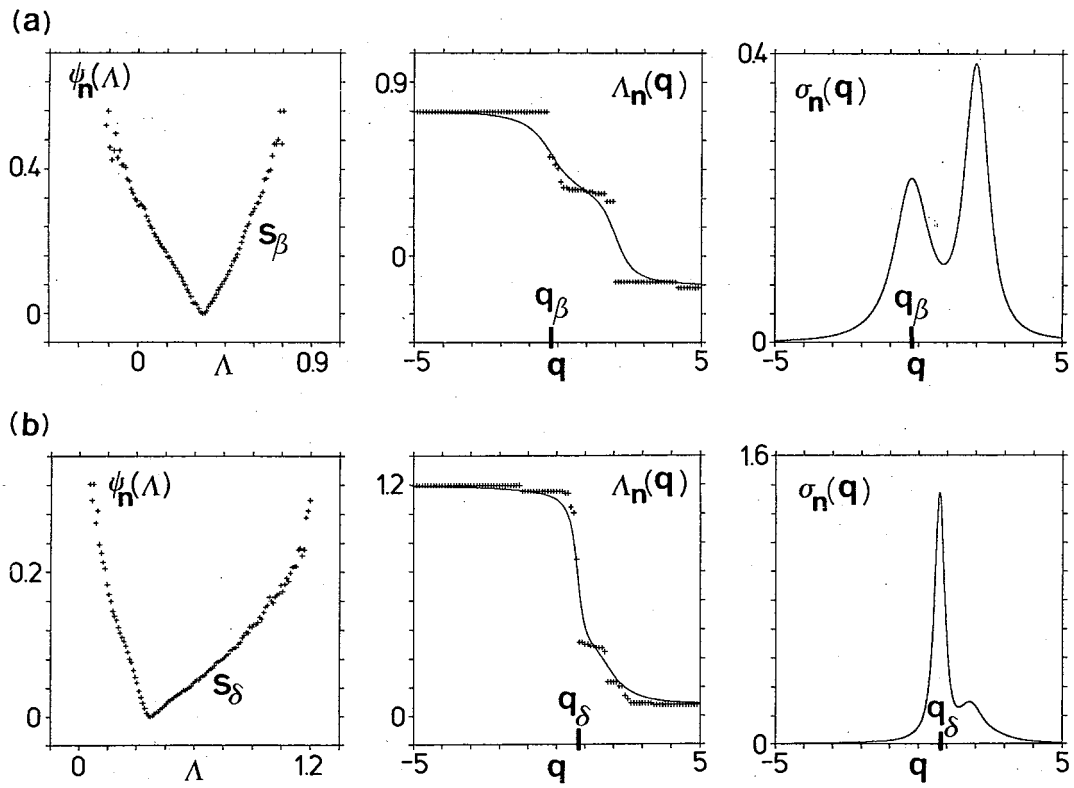

Fig. 7. Dynamic structure functions for the Duffing equation (3·1) near the crisis point $a=a_c$ with $\gamma=0.3$. (a) Just before the crisis, where $a=10.5242$, $n=18$, $N=3.2\times10^5$. (b) Just after the crisis, where $a=10.55$, $n=30$, $N=3.2\times10^5$.

q_β-phase transition with $q_\beta \simeq -0.24$ occurs in addition to the q_α-phase transition just before the crisis. The agreement between the theory and the numerical experiment for the slope $s_\beta = 1 - q_\beta$ is satisfactory, as listed in Table I. Just after the crisis a q_δ-phase transition occurs at $q = q_\delta \simeq 0.74$.

§ 4. A short summary and some remarks

In the present paper we have studied the q-phase transitions of the q-weighted average $\Lambda(q)$ of the coarse-grained expansion rates Λ for the ordinary differential equations, such as the driven damped pendulum and the Duffing equation. By taking the Poincaré maps of the differential equations, we have used the formalism for the q-phase transitions established for $2d$ maps. Numerically, it has been found that, although the chaotic attractors are much more complicated than those of simple $2d$ maps such as the Hénon map, the q_β- and q_δ-phase transitions occur in addition to the q_α-phase transition just before and after the crises, respectively, in the same way as in the Hénon map. Therefore, the q-phase transitions must be universal phenomena and observable even in other physical systems such as fluids.

The slopes s_β of $\psi(\Lambda)$ just before the crises are listed in Table I, where the agreement between theory and numerical experiments is satisfactory. On the other hand, the slopes s_δ of the q_δ-phase transition cannot be estimated theoretically except for type I intermittent chaos of a piecewise-linear Markov map[12] and the 3-band crisis of an asymmetric tent map.[20] Therefore, to obtain a theoretical expression for s_δ is an important problem and will be discussed elsewhere.

The q-weighted average $\alpha(q)$ of the singularity exponents α of the natural invariant measure is closely related to $\Lambda_\infty(q)$, so that if a q-phase transition occurs for $\Lambda_\infty(q)$ at a value $q = q_t$, then a q-phase transition also occurs for $\alpha(q)$ at a value $q = q_T$ given by

$$q_T = q_t + \Phi_\infty(q_t)/|\ln|J||\,, \tag{4·1}$$

as was studied for the Hénon map in Ref. 21). Therefore, it is important to study the q-phase transitions of $\alpha(q)$ for differential equations, which will be reported on a future occasion.

Acknowledgements

We wish to thank Professor Y. Ueda, Dr. T. Yoshida and all others of our chaos group at Kyushu University for stimulating and useful discussions. This study was partially financed by the Grant-in-Aid for Scientific Research of Ministry of Education, Science and Culture.

References

1) T. C. Halsey, M. H. Jensen, L. P. Kadanoff, I. Procaccia and B. I. Shraiman, Phys. Rev. **A33** (1986), 1141, and references quoted therein.
2) H. Fujisaka, Prog. Theor. Phys. **70** (1983), 1264; **71** (1984), 513.
3) M. Sano, S. Sato and Y. Sawada, Prog. Theor. Phys. **76** (1986), 945.

J. -P. Eckmann and I. Procaccia, Phys. Rev. **A34** (1986), 659.
4) H. Fujisaka and M. Inoue, Prog. Theor. Phys. **77** (1987), 1334.
G. Paladin and A. Vulpiani, Phys. Rep. **156** (1987), 147.
5) T. Morita, H. Hata, H. Mori, T. Horita and K. Tomita, Prog. Theor. Phys. **78** (1987), 511; **79** (1988), 296.
6) P. Grassberger, R. Badii and A. Politi, J. Stat. Phys. **51** (1988), 135.
7) H. Hata, T. Horita, H. Mori, T. Morita and K. Tomita, Prog. Theor. Phys. **80** (1988), 809.
8) T. Horita, H. Hata, H. Mori, T. Morita, K. Tomita, S. Kuroki and H. Okamoto, Prog. Theor. Phys. **80** (1988), 793.
9) T. Horita, H. Hata, H. Mori, T. Morita and K. Tomita, Prog. Theor. Phys. **80** (1988), 923.
10) K. Tomita, H. Hata, T. Horita, H. Mori and T. Morita, Prog. Theor. Phys. **80** (1988), 953.
11) K. Tomita, H. Hata, T. Horita, H. Mori and T. Morita, Prog. Theor. Phys. **81** (1989), 1.
12) N. Mori, T. Kobayashi, H. Hata, T. Morita, T. Horita and H. Mori, Prog. Theor. Phys. **81** (1989), 60.
13) R. S. Ellis, *Entropy, Large Deviations and Statistical Mechanics* (Springer-Verlag, New York, 1985).
14) C. Grebogi, E. Ott, F. Romeiras and J. A. Yorke, Phys. Rev. **A36** (1987), 5365.
15) A. H. MacDonald and M. Plischke, Phys. Rev. **B29** (1983), 201.
16) M. Octavio, Phys. Rev. **B29** (1984), 1231.
17) J. Guckenheimer and P. Holmes, *Nonlinear Oscillations, Dynamical Systems, and Bifurcations of Vector Field* (Springer, New York, 1983).
18) Y. Ueda, J. Stat. Phys. **20** (1979), 181.
19) D. Ruelle, The Mathematical Intelligencer (Springer-Verlag) **2** (1980), 126.
20) S. Miyazaki et al., private communication.
21) H. Hata, T. Horita, H. Mori, T. Morita and K. Tomita, Prog. Theor. Phys. **81** (1989), 11.